PROTEINS
STRUCTURE ■ FUNCTION ■ BIOINFORMATICS

Thermodynamic stability, unfolding kinetics, and aggregation of the N-terminal actin-binding domains of utrophin and dystrophin

Surinder M. Singh,[1] Justine F. Molas,[1] Narsimulu Kongari,[1] Swati Bandi,[1] Geoffrey S. Armstrong,[2] Steve J. Winder,[3] and Krishna M. G. Mallela[1]*

[1] Department of Pharmaceutical Sciences, Skaggs School of Pharmacy and Pharmaceutical Sciences, University of Colorado Anschutz Medical Campus, Aurora, Colorado 80045
[2] Department of Chemistry and Biochemistry, University of Colorado at Boulder, Boulder, Colorado 80309
[3] Department of Biomedical Science, University of Sheffield, Western Bank, Sheffield S10 2TN, United Kingdom

ABSTRACT

Muscular dystrophy (MD) is the most common genetic lethal disorder in children. Mutations in dystrophin trigger the most common form of MD, Duchenne, and its allelic variant Becker MD. Utrophin is the closest homologue and has been shown to compensate for the loss of dystrophin in human disease animal models. However, the structural and functional similarities and differences between utrophin and dystrophin are less understood. Both proteins interact with actin through their N-terminal actin-binding domain (N-ABD). In this study, we examined the thermodynamic stability and aggregation of utrophin N-ABD and compared with that of dystrophin. Our results show that utrophin N-ABD has spectroscopic properties similar to dystrophin N-ABD. However, utrophin N-ABD has decreased denaturant and thermal stability, unfolds faster, and is correspondingly more susceptible to proteolysis, which might account for its decreased *in vivo* half-life compared to dystrophin. In addition, utrophin N-ABD aggregates to a lesser extent compared with dystrophin N-ABD, contrary to the general behavior of proteins in which decreased stability enhances protein aggregation. Despite these differences in stability and aggregation, both proteins exhibit deleterious effects of mutations. When utrophin N-ABD mutations analogous in position to the dystrophin disease-causing mutations were generated, they behaved similarly to dystrophin mutants in terms of decreased stability and the formation of cross-β aggregates, indicating a possible role for utrophin mutations in disease mechanisms.

Proteins 2012; 80:1377–1392.

Key words: stability; unfolding; aggregation; disease; muscular dystrophy; dystrophin; utrophin; actin-binding domain; calponin-homology domain.

INTRODUCTION

Muscular dystrophy (MD) is a severe, debilitating group of neuromuscular diseases.[1] Duchenne (DMD) and Becker muscular dystrophies (BMD) account for more than half of all known MDs. These two diseases are caused by the loss of function of a vital muscle protein dystrophin[2] whose gene resides on the human X-chromosome. These dystrophin-related diseases physically weaken patients to a state of immobility, leading to death at an early age. Dystrophin stabilizes the muscle cell membrane against the mechanical forces associated with muscle stretch and contraction by connecting the actin filaments to the sarcolemmal transmembrane glycoprotein complex.[3–5] Mutations in dystrophin result in its loss of function.[6–11] Utrophin is a protein product of human chromosome 6 and is the closest autosomal homologue of dystrophin.[12–15] Utrophin has been shown to compensate for the loss of functional dystrophin in human disease animal models.[16–23] However, the underlying physical mechanisms and the structural and functional similarities and differences between utrophin and dystrophin are less understood.

Utrophin is confined specifically to the sarcolemma in fetal and regenerating muscle cells.[24–27] After down-regulation at

Additional Supporting Information may be found in the online version of this article.
Abbreviations: ABD, actin-binding domain; BMD, Becker MD; CD, circular dichroism; CH domain, calponin-homology domain; C_m, midpoint denaturant concentration in chemical denaturant melt; DMD, Duchenne MD; Dys, dystrophin; ΔG, Gibb's free energy; HSQC, heteronuclear single quantum coherence; K_d, dimer dissociation constant; *m*-value, the slope of ΔG variation with denaturant concentration; MD, muscular dystrophy; MRE, mean residue ellipticity; N, native state; N-ABD, N-terminal actin-binding domain; NMR, nuclear magnetic resonance; PK, proteinase K; T_m, midpoint temperature in thermal melt; U, unfolded state; Utr, utrophin; WT, wild-type.

Presented at the 24th Annual Symposium of the Protein Society, San Diego, CA, USA, August 2010 (See Ref. 112).
Grant sponsor: American Heart Association, Jane and Charlie Butcher grant in Genomics and Biotechnology, The ALSAM Foundation, Medical Research Council, UK.
*Correspondence to: Krishna M.G. Mallela, Department of Pharmaceutical Sciences, Skaggs School of Pharmacy and Pharmaceutical Sciences, University of Colorado Anschutz Medical Campus, Aurora, CO 80045. E-mail: krishna.mallela@ucdenver.edu
Received 13 July 2011; Revised 21 December 2011; Accepted 2 January 2012
Published online 9 January 2012 in Wiley Online Library (wileyonlinelibrary.com).
DOI: 10.1002/prot.24033

birth, it is found predominantly at the myotendinous and neuromuscular junctions in adult muscle cells to aid in optimal synapse transmission and to play a stabilizing role at these junctions.[15,28–31] Similar to dystrophin, utrophin is a long, rod-shaped protein, and is made up of 3433 amino acids (395 kDa). It has 60% sequence similarity and contains four distinct domains that are similar to dystrophin[5]: an N-terminal actin-binding domain (N-ABD) consisting of 261 residues, a central rod domain consisting of 22 spectrin repeats and four hinge regions, a cysteine-rich (CR) domain and a C-terminal (CT) domain. Utrophin interacts with actin using its N-ABD and the first 10 spectrin repeats in the central rod domain, and it interacts with the sarcolemma glycoprotein complex using its CR and CT domains.[5,15]

Considerable effort in recent years has been focused on understanding the functional and biochemical differences between utrophin and dystrophin. Utrophin has been shown to interact with dystrophin-associated proteins[32–35] and binds to actin similar to dystrophin.[34,36] However, clear marked differences exist between utrophin and dystrophin. Utrophin interacts with actin through a different contact surface compared with dystrophin,[36] binds to lesser number of actin monomers,[34,36] requires higher protein concentrations to protect actin filaments against depolymerization,[36] differentially affects the structural dynamics of actin,[37] and has a decreased *in vivo* half-life.[16,21,38,39] Some of these functional and biochemical differences between dystrophin and utrophin, in particular, their *in vivo* half-life, might originate from their differences in thermodynamic stability and unfolding. Dystrophin and utrophin are two large proteins containing more than 3400 amino acids, and hence they are not amenable to many structural and biophysical methods that measure protein stability and unfolding. Moreover, it is not yet possible to obtain high yields of highly pure proteins necessary for biophysical studies. Therefore, we followed a reductionist approach of studying individual domains, commonly used in protein structure–function studies. In this study, we examined whether the N-ABDs of dystrophin and utrophin differ in terms of their stability and unfolding. N-ABDs are of particular interest because their crystal structures are known,[40,41] and most disease-causing missense mutations that trigger MD occur in the N-ABD of dystrophin.[42,43]

Studying the stability of N-ABDs is also relevant in terms of improving the stability and *in vivo* half-life of the products of potential compensatory gene constructs such as utrophin itself, and mini- and micro-dystrophins and utrophins. Such constructs have been shown to compensate the loss of functional dystrophin in human disease mouse models,[16,17,22,23,44–50] and hold a high promise for future therapeutics to treat MD patients.[19,48,51–55] However, the products of these genes tend to have decreased stability, functionality, and decreased *in vivo* half-life[16,21,38,39,56,57] compared to the full-length dystrophin. All these proteins contain in common the N-ABD with which the proteins interact with F-actin and the C-terminal domains and the glycoprotein complex. Therefore, one method of stabilizing the proteins might be to increase the stability of the component domains, for example, that of N-ABDs. For this purpose, we need to first understand the stability and unfolding of dystrophin and utrophin N-ABDs that share a high sequence and structure similarity.

In addition, studying the stability of the N-ABDs might shed light onto the structural diversity and plasticity of tandem-calponin-homology (CH) domains.[58–63] Such a tandem array forms a major class of actin-binding domains in muscle proteins. Individual CH domains share a high sequence and structural similarity but differ in their mode of binding to actin. Such functional differences might originate from their differences in stability which might dictate the various dynamic conformations available for individual CH domains. This article examines the stability differences between the N-ABDs of dystrophin and utrophin, which are tandem CH-domains and are known to bind to actin with different modes of contact.[36,40,41,64]

MATERIALS AND METHODS

Protein expression and purification

N-ABDs of human utrophin (residues 1–261) and dystrophin (residues 1–246, C10S, C188S) cDNA were cloned into a pET28a (N-terminal His tag; Novagen) expression vector using NdeI and HindIII restriction sites and transformed into DH5α (Invitrogen) by the heat shock method. Three different mutants in utrophin N-ABD (L70R, A84D, and Y246N) were constructed using the Quick Mutagenesis protocol (Stratagene). Plasmid sequences of N-ABDs of dystrophin, utrophin, and its mutants were confirmed by DNA sequencing. These expression vectors were transformed into BL21-DE3 by the heat shock method. Cells were grown in 2 L of Luria broth (LB) and protein expression was induced with 0.5 m*M* isopropyl β-D-thiogalactopyranoside (IPTG) at a cell density corresponding to an optical density of 0.6 and incubated for 5 hr at 37°C. Cell pellet was harvested and used for protein purification. For utrophin and dystrophin N-ABDs, the cell pellet was resuspended in 50 m*M* Tris, 200 m*M* NaCl, pH 7.5, 1 m*M* phenylmethylsulfonyl fluoride (PMSF; protease inhibitor) buffer and sonicated with the samples kept on ice. Lysed suspension was centrifuged at 30,000*g* at 4°C for 40 min. Clear supernatant was loaded onto a Ni Sepharose Fast Flow column (GE Lifesciences) and bound protein was eluted with an imidazole gradient. Purity of elutes was evaluated using reducing SDS-PAGE. Pure elutes were pooled and dialyzed against PBS buffer (0.1*M* NaH_2PO_4, 0.15*M* NaCl,

pH 7). In the case of mutant purification, the post-sonication pellet containing inclusion bodies was washed twice with 50 m*M* Tris, 1 m*M* PMSF, 0.2*M* NaCl, 0.5 % Triton X-100, pH 7.5, and with double distilled water. The cell pellet was solubilized in 10 mL of solubilization buffer (8*M* urea, 0.2*M* NaCl, 50 m*M* Tris, pH 7.5) and incubated at room temperature for 30 min. Solubilized suspension was centrifuged at 30,000*g* for 30 min at 15°C. Clear supernatant was used for the Ni-affinity column and eluted with the imidazole gradient in the above solubilization buffer. Purity of elutes was checked on reducing SDS-PAGE gel. Pure elutes were pooled and dialyzed against PBS buffer (0.1*M* NaH_2PO_4, 0.15*M* NaCl, pH 7). Mutant aggregates in the dialysate were washed with PBS and were used for further experiments.

For labeling utrophin N-ABD with ^{15}N for heteronuclear NMR experiments, the cell pellet from 2 L of LB culture (optical density ~2) was resuspended in 1 L of sterile minimal media (48 m*M* Na_2HPO_4, 22 m*M* KH_2PO_4, 8.5 m*M* NaCl, 18.6 m*M* $^{15}NH_4Cl$, 2 m*M* $MgSO_4$, 0.1 m*M* $CaCl_2$, 0.4% glucose) and grown for 2 hr at 37°C. Protein expression was induced with 0.5 m*M* IPTG and incubated overnight. Labeled utrophin N-ABD was purified using Ni-affinity column chromatography.

Fluorescence and CD

Fluorescence spectra of native and unfolded states (in 8*M* urea) of utrophin and dystrophin N-ABDs (1 μ*M* each in PBS buffer) were recorded by exciting the samples at 280 nm (Fluoromax3, SPEX). CD spectra were recorded on an Applied Photophysics ChirascanPlus spectrometer.

Mean residue ellipticity (MRE) of the proteins were calculated from the CD values in millidegrees using the equation[65]

$$[\theta] = \text{millidegrees}/(\text{path length in millimeters} \times \text{molar concentration of protein} \times \text{number of residues}) \quad (1)$$

NMR experiments

Labeled protein (150 μ*M*) was used for recording 2D $^{15}N/^{1}H$ TROSY-HSQC spectra on a 900 MHz Varian NMR spectrometer (Rocky Mountain NMR Facility). Data were processed using NMRPipe software.[66] For longitudinal (T_1) and transverse (T_2) relaxation measurements, modified pulse sequences available with the Varian Biopack were used. Rotational correlation time, τ_c was calculated using the equation, $\tau_c = \frac{1}{4\pi\nu_N}\left(\sqrt{\frac{6T_1}{T_2} - 7}\right)$ where ν_N is the ^{15}N resonance frequency.

Chemical denaturant melts

Utrophin and dystrophin N-ABDs (1 μ*M*) in PBS buffer were used to monitor changes in the CD signal at 222 nm (ChirascanPlus spectrometer; Applied Photophysics, UK) and protein fluorescence with excitation at 280 nm (PTI QuantaMaster Fluorometer) with increasing urea (Nacalai Tesque, 35940-81) concentration. For this experiment, buffer samples with varying urea concentration were initially prepared and the protein was added from a stock solution. The samples were allowed to equilibrate for 1 hr. The data were normalized from 0 to 1 and fitted to a two-state model[67,68] using the SigmaPlot software (Systat Software Inc) to obtain the ΔG and *m*-values. We confirmed that the samples have reached equilibrium within 1 hr by recording the denaturant melt of 1 μ*M* dystrophin N-ABD equilibrated overnight and found no change in the ΔG and *m*-values. To confirm the absence of a dimer (K_d = 4 μ*M*) suspected in earlier published X-ray study on dystrophin N-ABD,[41] we performed denaturant melts at two protein concentrations (1 and 10 μ*M*) and found no change (Supporting Information Figure).

Thermal melts

For utrophin and dystrophin N-ABDs (1 μ*M* each in PBS buffer), changes in the far-UV CD signal at 222 nm and protein fluorescence with excitation at 280 nm (ChirascanPlus spectrometer, Applied Photophysics, UK) were monitored as a function of increasing temperature at a rate of 1°C/min. For mutants (~1 μ*M*), the CD signal was recorded at 208 nm. The data were fit to a two-state equilibrium unfolding model by using SigmaPlot software to determine the T_m values.

Stopped flow

Unfolding kinetics of utrophin and dystrophin N-ABDs were monitored using an Applied Photophysics stopped flow assembly attached to a ChirascanPlus spectrometer. Native N-ABDs (10 μ*M* each) were diluted 10 times into PBS buffer containing varying concentrations of urea, and the changes in the CD signal at 222 nm and the total protein fluorescence with excitation at 280 nm were recorded. An average of 20 traces was fit to exponential functions using SigmaPlot to determine the rate constants. The equation used for fitting the kinetic data to a multiexponential function was

$$y = y_0 + \sum_{i=1}^{n} a_n(1 - \exp(-k_n t)) \quad (2)$$

where k_n and a_n represent the rate constants and the corresponding signal amplitudes. In the above equation, $n = 2$ for two-exponential and $n = 3$ for three-exponential functions. The amplitude-weighted average rate constant was determined using the equation

$$\langle k \rangle = \left(\left(\sum_{i=1}^{n} |a_n|/k_n\right) \Big/ \sum_{i=1}^{n} |a_n|\right)^{-1}. \quad (3)$$

For monitoring aggregation kinetics, unfolded N-ABDs (100 μ*M*, PBS buffer, 8*M* urea) were diluted 10 times into PBS buffer without denaturant using a stopped flow mixer, and the changes in the right-angle light scattering with 450 nm excitation were monitored. An average of 10 traces was plotted using SigmaPlot. At the end of the reaction, the amount of refolded proteins was estimated by centrifuging the solutions at 30,000*g* for 1 hr at 4°C to remove insoluble aggregates and using the molar extinction coefficients at 280 nm calculated using the ExPASy program (http://ca.expasy.org/) as 46,075 M^{-1} cm^{-1} and 38,960 M^{-1} cm^{-1} for dystrophin and utrophin N-ABD, respectively.

Protease assay

Proteins (30 μg in 20 μL) were digested with a non-specific protease proteinase K (PK) at 37°C. To obtain the extent of proteolysis of the two proteins, the concentration of PK was varied from 0 to 100 ng and the reaction was carried out for 30 min. To obtain the kinetics of proteolysis of the two proteins, we fixed the PK concentration at 10 ng and the reaction time was varied from 0 to 190 min. Digestion reaction was stopped by adding 20 μL of reducing SDS-PAGE loading buffer. Samples were denatured by heating for 5 min at 100°C, centrifuged at 20,000*g* for 5 min, and the supernatant was loaded on the SDS-PAGE gel and stained with Coomassie Blue. The intensity of the individual bands was determined using the Quantity One software on Biorad Gel Doc XR+ instrument.

Dye-binding assays

Aggregates of utrophin N-ABD WT and mutants (2 μ*M* aggregated protein) and 50 μ*M* dye concentration were used for dye-binding studies. Thioflavin T fluorescence spectra were recorded using a Fluoromax3 fluorometer (SPEX) with 440 nm excitation. Congo red absorption spectra were recorded using an Agilent spectrophotometer.

RESULTS

Amino acid sequence and structural comparison of utrophin and dystrophin N-ABDs

Compared with full-length proteins which have 60% sequence similarity,[5] N-ABDs share 82% sequence similarity [Fig. 1(A)] when aligned using the ClustalW2 program[69] (http://www.ebi.ac.uk/Tools/msa/clustalw2/). Earlier X-ray crystal structures[40,41] indicate that these domains contain two calponin-homology binding (CH) domains connected by an α-helix [Fig. 1(B)]. When aligned using the MultiProt program[70] (http://bioinfo3d.cs.tau.ac.il/MultiProt/), clear differences can be seen between the two N-ABDs [Fig. 1(C)]. The relative orientation of the two CH domains around the central α-helix is distinctly different for the two N-ABDs, although the two CH domains of utrophin are highly similar in structure to the corresponding CH domains from dystrophin [Fig. 1(D).

Biophysical characterization of utrophin N-ABD

Similar to dystrophin N-ABD,[42] we were able to obtain high yields of highly pure utrophin N-ABD by expressing it in *E. coli* and purifying it using the metal affinity method [Fig. 2(A)]. Utrophin N-ABD consists of 261 residues, whereas dystrophin N-ABD has 246 residues; hence, utrophin N-ABD appears as a slightly higher molecular weight band on the SDS-PAGE gel [Fig. 2(A)]. Utrophin N-ABD has similar spectroscopic characteristics to those of dystrophin N-ABD. The circular dichroism (CD) spectrum shows two negative bands at 208 and 222 nm characteristic of an α-helical structure [Fig. 2(B)], consistent with its crystal structure [Fig. 1(B)]. In addition, the native fluorescence of utrophin N-ABD is blue shifted with respect to its unfolded state (U) [Fig. 2(C)], similar to dystrophin N-ABD. The native fluorescence emission maximum occurs at 334 and 338 nm for utrophin and dystrophin N-ABDs, respectively, whereas the unfolded state fluorescence maximum occurs at 355 nm for both proteins. The blue shift in the tryptophan emission maximum of the native state indicates the burial of tryptophan residues from the solvent.[71] For tryptophans that are exposed to solvent, this emission maximum occurs at around 355 nm, whereas for tryptophans buried in the protein interior, the emission maximum occurs at around 325 nm. The observed blue shift of 21 nm for native utrophin N-ABD indicates that at least some of the six conserved tryptophan residues are significantly buried in the protein interior, implying that the protein has a well-folded structure.

Two-dimensional ^{15}N-^{1}H HSQC NMR spectrum [Fig. 2(D)] is consistent with the above spectroscopic observations that the utrophin N-ABD has a well-folded structure in solution. The crosspeaks between amide nitrogens and hydrogens are well-resolved on both ^{15}N and especially ^{1}H chemical shift scale, indicating that the individual nuclear spins experience distinct structural environments in the protein, characteristic of a well-defined protein structure. For an unfolded or molten globule-like protein, amide crosspeaks will be in general clustered in a single chemical shift region, in particular along the ^{1}H chemical shift scale. In addition, the average tumbling time or the rotational correlation time (τ_c) calculated from the longitudinal (T_1) and transverse (T_2) relaxation rates of individual amides indicates that the protein is a monomer in solution

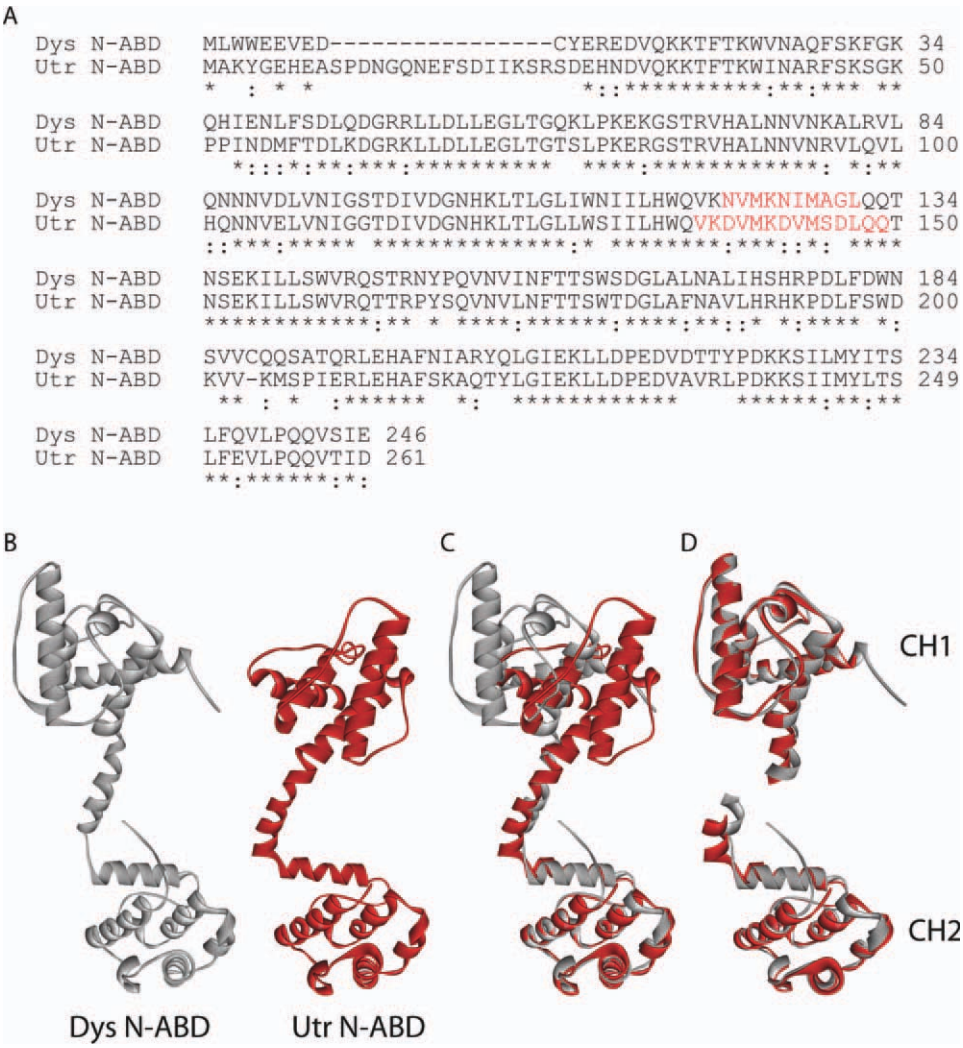

Figure 1

Sequence and structural comparison of the N-ABDs. **A**. Amino acid sequence alignment of the N-ABDs of human dystrophin (Dys; DMD gene product) and utrophin (Utr; UTRN gene product) using the ClustalW2 program[69] (http://www.ebi.ac.uk/Tools/msa/clustalw2/). Residues marked with an asterisk (*) indicate identical residues and those marked with a colon (:) indicate highly conserved residues. Red colored residues show the α-helix connecting the two CH domains. **B**. X-ray crystal structures of dystrophin (Dys) and utrophin (Utr) N-ABDs.[40,41] **C**. Structural alignment of the N-ABDs using the MultiProt program[70] (http://bioinfo3d.cs.tau.ac.il/MultiProt/). **D**. Structural alignment of the corresponding CH1 (N-terminal) and CH2 (C-terminal) domains in the two N-ABDs using the MultiProt program. In panels B–D, gray and red colored structures represent dystrophin and utrophin N-ABDs, respectively. Molecular structures were drawn using the program Accelrys Discovery Studio Visualizer (http://accelrys.com/products/discovery-studio/visualization-download.php).

[Fig. 2(E)]. For a spherical protein with a similar chain length to that of utrophin N-ABD, the expected correlation time is 17 ns,[72] whereas the experimentally measured correlation time was 19 ns. The slightly higher τ_c observed suggests that the protein might be somewhat nonspherical. These NMR results in addition to CD and fluorescence confirm that the utrophin N-ABD is a well-folded monomer in solution, in agreement with the earlier structural and functional studies.[30,33,40,64] Similar results were observed for dystrophin N-ABD,[42] which indicate that it is also a monomer in solution.

Utrophin N-ABD is less stable than dystrophin N-ABD

Despite having high sequence and structural similarity to dystrophin N-ABD (Fig. 1), utrophin N-ABD has a decreased thermodynamic stability [Figs. 3(A–D)]. When equilibrium protein unfolding was measured using the chemical denaturant urea which destabilizes the native protein structure, utrophin N-ABD unfolded at lower urea concentrations than did dystrophin N-ABD [Figs. 3(A,B)]. When CD at 222 nm was used to monitor the unfolding of the secondary structure (α-helices) of

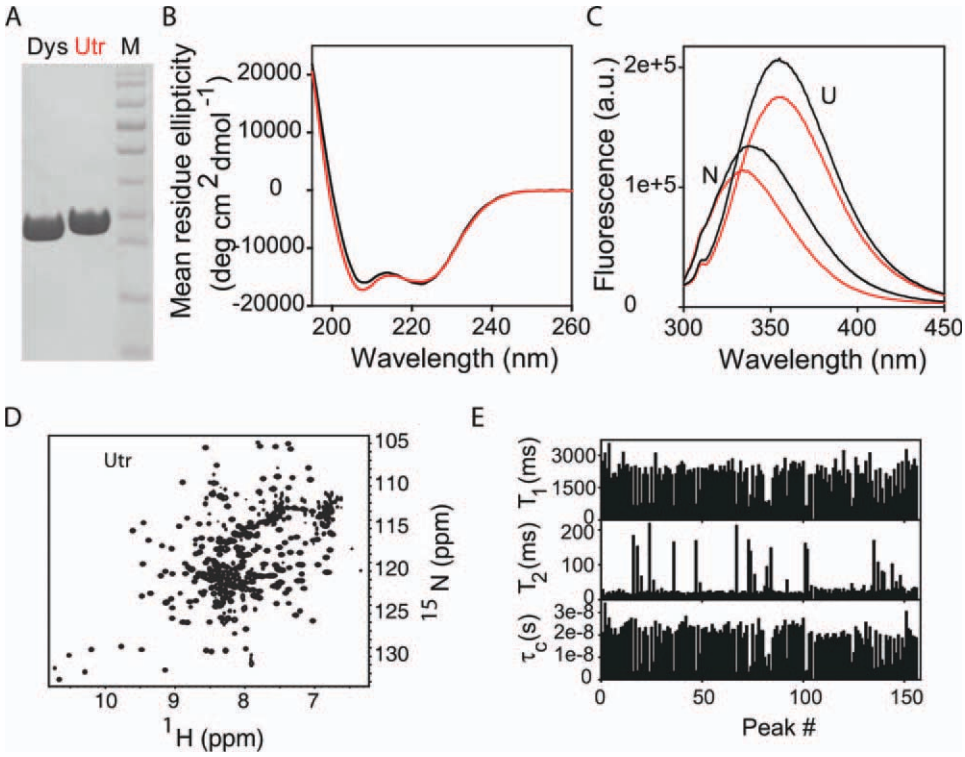

Figure 2

Biophysical characterization of the N-ABDs. **A**. SDS-PAGE of purified utrophin and dystrophin N-ABDs. Lanes Dys and Utr correspond to dystrophin and utrophin N-ABDs, respectively. Lane M corresponds to the protein molecular weight markers (bottom to top: 11, 17, 26, 34, 43, 56, 72, 96, 130, and 170 kDa, respectively). **B**. CD spectra of native proteins. **C**. Fluorescence spectra of native (N) and unfolded (U) states. Black and red curves in panels B and C correspond to dystrophin and utrophin N-ABDs, respectively. **D**. 2D ^{15}N-^{1}H TROSY-HSQC NMR spectrum of utrophin N-ABD. **E**. T_1, T_2, and τ_c values for individual amide crosspeaks of utrophin N-ABD (arbitrarily numbered, because the residue assignments are not known at present). In this calculation, only strong and nonoverlapping peaks were considered. [Color figure can be viewed in the online issue, which is available at wileyonlinelibrary.com.]

the protein [Fig. 3(A)], utrophin N-ABD consistently melted at 1.3*M* [urea] units lower than that of dystrophin N-ABD. Fitting the melting curves to a two-state equation[67,68] resulted in $\Delta G = 5.44 \pm 0.30$ kcal/mol and $m = -1.22 \pm 0.06$ kcal/mol/*M* [urea] for utrophin N-ABD, and $\Delta G = 9.81 \pm 0.55$ kcal/mol and $m = -1.68 \pm 0.10$ kcal/mol/*M* [urea] for dystrophin N-ABD (Table I). These free energy values indicate that utrophin N-ABD is less stable than dystrophin by 4.4 kcal/mol. In addition, utrophin N-ABD has a lesser *m*-value compared to dystrophin N-ABD. The *m*-value in denaturant melts is a measure of the amount of accessible surface area exposed upon unfolding,[73] which indicates that utrophin N-ABD might be less compact compared to dystrophin N-ABD.

Similar results were obtained when protein fluorescence was used to monitor the unfolding [Fig. 3(B)], which is often considered as a probe for the tertiary structure of a protein. Utrophin N-ABD consistently unfolded at 1.5*M* [urea] units lower than dystrophin N-ABD. The ΔG and *m*-values obtained by fitting these curves to a two-state equation[67,68] were $\Delta G = 7.79 \pm 0.25$ kcal/mol and $m = -1.80 \pm 0.06$ kcal/mol/*M* [urea] for utrophin N-ABD, and $\Delta G = 12.84 \pm 0.77$ kcal/mol and $m = -2.23 \pm 0.13$ kcal/mol/*M* [urea] for dystrophin N-ABD, respectively (Table I). These values indicate that the utrophin N-ABD is less stable than dystrophin N-ABD by 5.1 kcal/mol when measured by fluorescence, and the *m*-values indicate that utrophin N-ABD is less compact compared to dystrophin N-ABD. These results qualitatively agree with the above conclusions drawn from CD measurements [Fig. 3(A)]. However, the ΔG and *m*-values obtained from CD and fluorescence measurements do not match, indicating that the two proteins do not follow a two-state unfolding mechanism. If a protein is a two-state folder, i.e., there exists only native (N) and unfolded (U) states with no partially unfolded intermediates, we expect to observe the same ΔG and *m*-values irrespective of the probe used to monitor unfolding. The disagreement between the ΔG and *m*-values measured by CD and fluorescence indicates that partially unfolded intermediates do exist between the N and U states and populate at equilib-

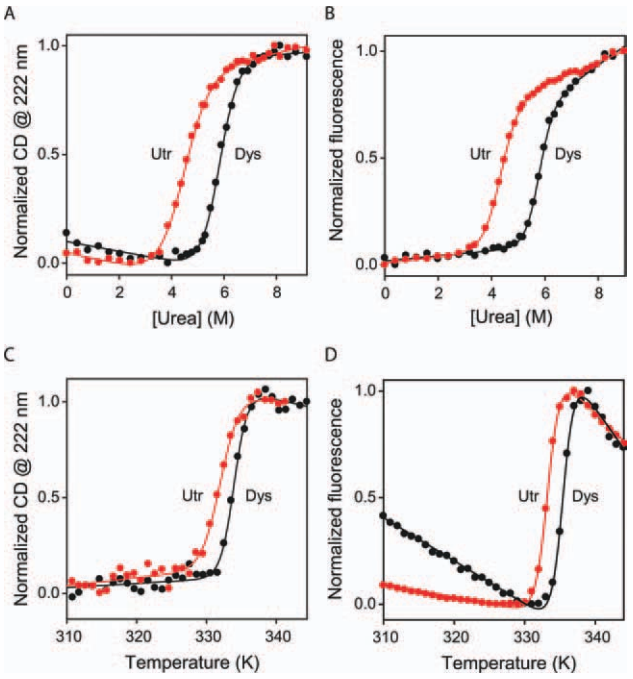

Figure 3

Protein stability measured using urea and temperature melts. **A**. Changes in the CD signal at 222 nm. **B**. Changes in the protein fluorescence with excitation at 280 nm as a function of urea concentration. **C**. Changes in the CD signal at 222 nm. **D**. Changes in the protein fluorescence with excitation at 280 nm as a function of increasing solution temperature. In all the panels, black and red curves correspond to dystrophin (Dys) and utrophin (Utr) N-ABDs, respectively. [Color figure can be viewed in the online issue, which is available at wileyonlinelibrary.com.]

rium. Since the ΔG and *m*-values measured by fluorescence are higher than those measured by CD, they might represent a close approximation of the true ΔG and *m*-values of the proteins.

Denaturant *m*-values can be used to estimate the compactness of protein structure. As described above, the *m*-value is proportional to the accessible surface area.[73] X-ray crystal structures of the two N-ABDs [Fig. 1(B)] were used to calculate the accessible surface area of the native states (using the program Accelrys Discovery Studio Visualizer) as 13,311 and 13,145 Å^2 for utrophin and dystrophin N-ABDs, respectively. Using the empirical equation, urea *m*-value (cal/mol/*M* [urea]) = 374 + 0.11 (ΔASA),[73] we calculated the *m*-values as −1.84 kcal/mol/*M* [urea] and −1.82 kcal/mol/*M* [urea] for utrophin and dystrophin N-ABDs, respectively. This estimated *m*-value for utrophin N-ABD closely matches with the −1.80 kcal/mol/*M* [urea] determined from urea melt measured by fluorescence (Table I), indicating that the conformation of utrophin N-ABD in solution might be similar to that in the X-ray structure [Fig. 1(B)]. However, the measured *m*-value (−2.23 kcal/mol/*M* [urea]) for dystrophin N-ABD is much higher than the estimated *m*-value (−1.82 kcal/mol/*M* [urea]), implying that the solution state structure of dystrophin N-ABD might be much more compact (by about 41%) than that in the X-ray crystal structure.

Temperature melts are commonly used in literature rather than the chemical denaturant melts to measure the thermodynamic stability of dystrophin and utrophin variants,[42,43,56,74–76] because the thermal melts require less protein (one protein sample) compared to the multiple protein samples (prepared at different chemical denaturant concentrations) required for denaturant melts. However, the results obtained from thermal melts have to be analyzed with caution because these melts are not reversible and should be interpreted on a qualitative rather than on a quantitative scale. With temperature as the destabilizing agent and either CD [Fig. 3(C)] or fluorescence [Fig. 3(D)] as the optical signal, utrophin N-ABD melted with a midpoint temperature (T_m) of 2°C less than that of dystrophin N-ABD (Table I), indicating that utrophin N-ABD is less stable than dystrophin N-ABD even at higher temperatures.

To confirm the absence of a dimeric form with a K_d of 4 μ*M* suspected in earlier studies on dystrophin N-ABD,[41] we measured denaturant melts at two different protein concentrations (Supporting Information Figure). The melt recorded at 10 μ*M* protein concentration exactly overlapped with that recorded at 1 μ*M* protein concentration, indicating the absence of dimer under our experimental conditions. Consistently, all our experiments were performed at native protein concentrations below 10 μ*M*, except protein NMR [Figs. 2(D,E)].

Utrophin N-ABD unfolds faster than dystrophin N-ABD

The unfolding of N-ABDs was initiated by diluting the native proteins (10 μ*M*) in the absence of denaturant into a high denaturant buffer (8*M* urea) by 10 times using a stopped flow mixer. The kinetics was followed by measuring changes in the CD signal at 222 nm to monitor the unfolding of the secondary structure (α-helices) of proteins [Figs. 4(A,B)]. These unfolding curves do not follow single exponential kinetics and were fitted to a two-exponential function [Eq. (2)] to obtain the unfolding rates. When monitored by CD, utrophin N-ABD unfolded with two unfolding rate constants of 15.34 ± 0.60 and 0.30 ± 0.02/s (relative amplitudes of 43.8% and 56.2%, respectively) [Fig. 4(B) and Table I], whereas dystrophin N-ABD unfolded with the rate constants of 2.81 ± 0.11 and 0.13 ± 0.01/s (relative amplitudes 44.1% and 55.9%) [Fig. 4(A) and Table I]. Comparing the individual rate constants having similar amplitude, it is clear that the secondary structure of utrophin N-ABD unfolds faster than that of dystrophin N-ABD. The unfolding experiment was repeated at varying urea con-

Table I
Equilibrium and Kinetic Parameters Obtained from Protein Melts (Fig. 3), Unfolding Kinetics (Fig. 4), and Protease Assays (Fig. 5) of Utrophin and Dystrophin N-ABDs

Equilibrium/kinetic parameter	Utr N-ABD	Dys N-ABD
Urea melt [Figs. 3(A,B)]		
CD [Fig. 3(A)]		
ΔG (kcal/mol)	5.44 ± 0.30	9.81 ± 0.55
m (kcal/mol/M [urea])	−1.22 ± 0.06	−1.68 ± 0.10
Fluorescence [Fig. 3(B)]		
ΔG (kcal/mol)	7.79 ± 0.25	12.84 ± 0.77
m (kcal/mol/M [urea])	−1.80 ± 0.06	−2.23 ± 0.13
Thermal melt [Figs. 3(C,D)]		
T_m (K) [CD; Fig. 3(C)]	332.1 ± 0.3	334.0 ± 0.1
T_m (K) [Fluorescence; Fig. 3(D)]	333.3 ± 0.1	335.4 ± 0.1
Unfolding kinetics (Fig. 4)		
CD [Figs. 4(A–C)]		
k_n (/s) (relative amplitudes) (8*M* urea)	15.34 ± 0.60 (43.8%) 0.30 ± 0.02 (56.2%)	2.81 ± 0.11 (44.1%) 0.13 ± 0.01 (55.9%)
$\langle k \rangle$ (/s) (8*M* urea)	0.53	0.22
m_u (kcal ln(/s)/mol/M [urea])	0.31 ± 0.03 0.11 ± 0.01	0.28 ± 0.03 0.12 ± 0.02
Fluorescence [Figs. 4(D–F)]		
k_n (/s) (relative amplitudes) (8*M* urea)	10.38 ± 0.63 (12.7%) 0.36 ± 0.01 (87.3%)	32.84 ± 2.98 (8.6%) 1.65 ± 0.18 (12.0%) 0.16 ± 0.004 (79.4%)
$\langle k \rangle$ (/s) (8*M* urea)	0.41	0.20
m_u (kcal ln(/s)/mol/*M* [urea])	0.24 ± 0.03 0.14 ± 0.02	0.06 ± 0.18 −0.07 ± 0.04 0.15 ± 0.02
Proteinase K assay (Fig. 5)		
PK_{50} (ng) [Figs. 5(B,D)]	11.9 ± 1.3	23.7 ± 2.6
$k_{proteolysis}$ (/min/10 ng [PK]; Figs. 5(F,H))	0.010 ± 0.002	0.005 ± 0.001

centrations, and the changes in the unfolding rate constants with urea concentration (unfolding chevron plot) was plotted in Figure 4(C). The measured rate constants indicate that utrophin N-ABD consistently unfolded at a much faster rate compared to dystrophin N-ABD at all urea concentrations.

When the same unfolding was monitored by protein fluorescence under identical conditions [Figs. 4(D,E)], the unfolding kinetics of dystrophin and utrophin N-ABDs follow multiexponential kinetics, similar to when measured by CD [Figs. 4(A–C)]. At 8*M* urea, utrophin N-ABD unfolds with two rate constants 10.38 ± 0.63 and 0.36 ± 0.01/s (relative amplitudes of 12.7% and 87.3%, respectively) [Fig. 4(E) and Table I], whereas dystrophin N-ABD unfolds with three rate constants 32.84 ± 2.98, 1.65 ± 0.18, and 0.16 ± 0.01/s (relative amplitudes of 8.6%, 12.0%, and 79.4%, respectively) [Fig. 4(D) and Table I]. Comparing the rate constant with maximum amplitude (0.36 vs. 0.16/s) or the amplitude weighted average rate constant [0.41 and 0.20/s for utrophin and dystrophin N-ABDs, respectively; Eq. (3) and Table I], utrophin N-ABD unfolded faster than dystrophin N-ABD by at least two times. The same phenomenon was observed when the experiment was performed at varying denaturant concentrations. At all urea concentrations, utrophin N-ABD unfolded faster than dystrophin N-ABD [Fig. 4(F); compare red circles with black circles]. The slowest rate constant is always of the maximum amplitude in both N-ABDs when measured by fluorescence and its amplitude qualitatively appears similar to an unfolding melt [Fig. 3(B)]. Hence, this rate constant might correspond to the population growth kinetics of the unfolded state with increase in the denaturant concentration. Since dystrophin N-ABD shows three-exponential unfolding kinetics, there exist at least two partially unfolded intermediates between the native and unfolded states. For any kinetic system containing n species, the maximum number of rate constants that can be observed will be n-1.[77] Similarly the two unfolding rate constants for utrophin N-ABD indicate that there exist at least one intermediate between the N and U states.

Utrophin N-ABD is more prone to proteolysis than dystrophin N-ABD

A nonspecific protease proteinase K (PK) was used to examine the proteolytic susceptibility of the two proteins. In the first experiment [Figs. 5(A,C)], the two N-ABDs were subjected to proteolysis at increasing concentration of PK for 30 min at 37°C. The band intensity corre-

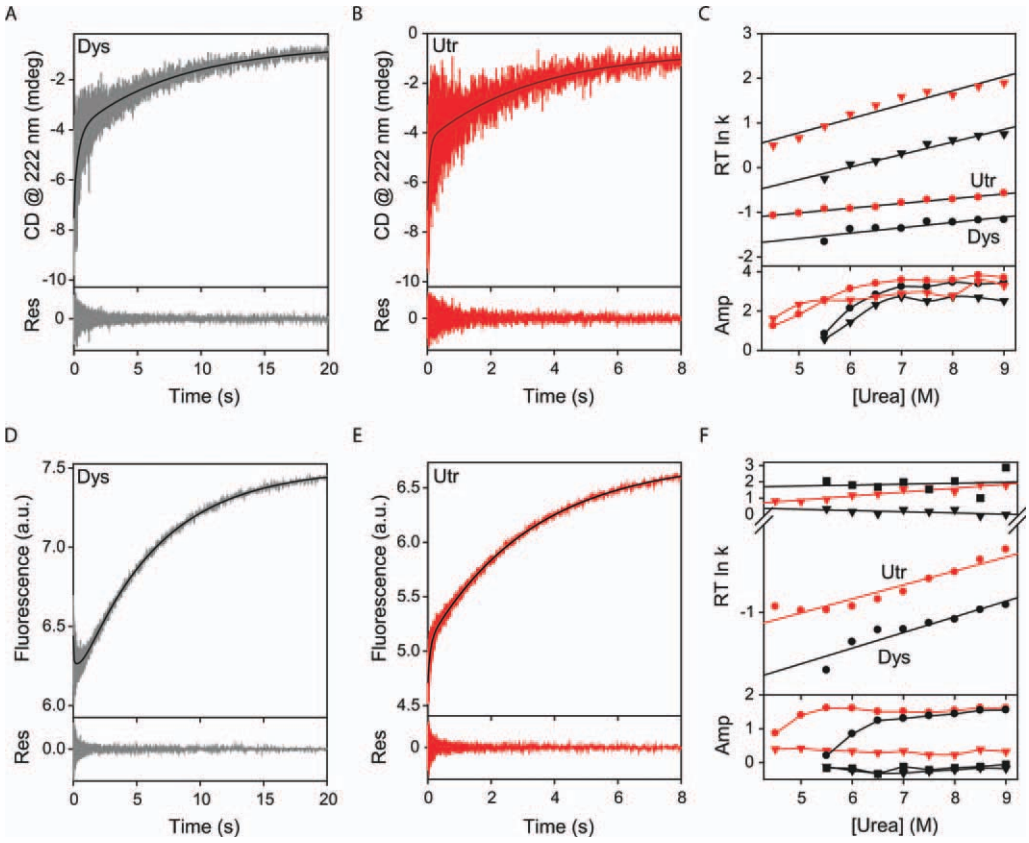

Figure 4

Unfolding kinetics of the N-ABDs. Panels **A** and **B** show the unfolding kinetics in 8*M* urea when measured by CD signal at 222 nm. Panel **C** shows the variation in the unfolding rate constants and their amplitudes with urea concentration. Panels **D** and **E** show the unfolding kinetics in 8*M* urea when monitored by protein fluorescence. Panel **F** shows the variation in the rate constants and respective amplitudes with urea concentration. In all panels, black and red colored symbols represent the data corresponding to dystrophin (Dys) and utrophin (Utr) N-ABDs, respectively. [Color figure can be viewed in the online issue, which is available at wileyonlinelibrary.com.]

sponding to the native utrophin N-ABD decreased with increasing protease concentration at a faster rate compared with that of dystrophin N-ABD [comparing the intensities of the bands inside the black boxes in Figures 5(A,C); plotted in Figures 5(B,D) respectively], indicating that utrophin N-ABD is more prone to proteolysis than dystrophin N-ABD. The data were fitted to a single exponential function to estimate the effective protease concentration that gave 50% degradation (PK_{50})[78] under the conditions used (Table I). The PK_{50} values were 11.9 $\pm$ 1.3 and 23.7 $\pm$ 2.6 ng for utrophin and dystrophin N-ABDs, respectively, which indicate that utrophin N-ABD requires less protease concentration for its proteolysis compared to dystrophin N-ABD. In the second set of experiments [Figs. 5(E,G)], the two proteins were subjected to proteolysis for varying amounts of time at a fixed concentration (10 ng) of PK. With the increase in reaction time, utrophin N-ABD band intensity decreased at a faster rate when compared with dystrophin N-ABD [Figs. 5(F,H)]. The rate constants obtained by fitting these kinetic data to a single exponential function were 0.010 $\pm$ 0.002 and 0.005 $\pm$ 0.001/min for utrophin and dystrophin N-ABDs, respectively. These rate constants indicate that utrophin N-ABD is more prone to proteolysis compared to dystrophin N-ABD, consistent with the conclusions drawn earlier [Figs. 5(A–D)].

The proteolysis pattern also differs between the two N-ABDs. At longer digestion times or at higher protease concentrations, dystrophin N-ABD proteolyses into two smaller fragments [Figs. 5(A,E)], whereas a major fraction of the utrophin N-ABD exists as a larger molecular weight fragment [Figs. 5(C,G)], which indicates inherent differences in the stabilities of the local protein regions[79] between the two N-ABDs.

Utrophin N-ABD aggregates less than dystrophin N-ABD

No aggregation was seen for native utrophin N-ABD at room temperature, similar to dystrophin N-ABD.[42]

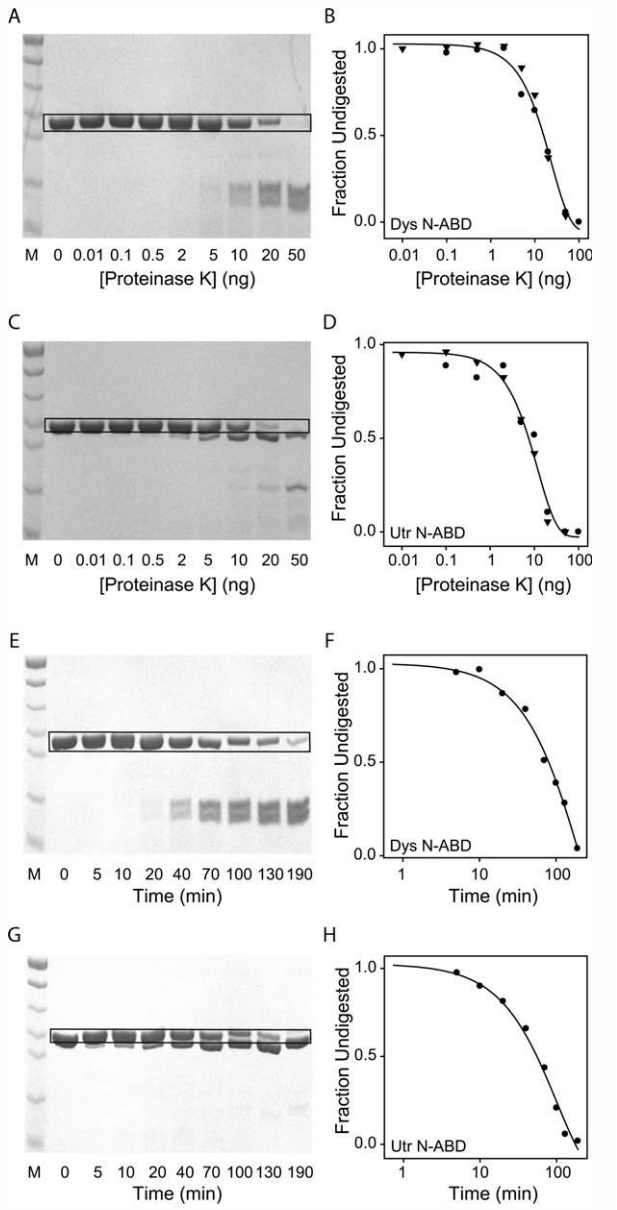

Figure 5

SDS-PAGE of the N-ABDs digested with proteinase K. Panels **A** and **B** show the proteolysis of dystrophin N-ABD, whereas panels **C** and **D** show the proteolysis of utrophin N-ABD as a function of increasing proteinase K concentration. The reaction was carried out at 37°C for 30 min. In panels **B** and **D**, circles and triangles represent two independent data sets. Panels **E** and **F** show the proteolysis of dystrophin N-ABD, whereas panels **G** and **H** show the proteolysis of utrophin N-ABD as a function of increasing reaction time at 37°C and with 10 ng proteinase K concentration. In all gel pictures, lane M corresponds to the protein molecular weight markers (bottom to top: 11, 17, 26, 34, 43, 56, and 72 kDa, respectively). For obtaining the undigested fractions shown in panels **B**, **D**, **F**, and **H**, the intensity of the band corresponding to the native proteins inside the black colored boxes was used.

Therefore, to monitor the aggregation propensity of these two proteins, we unfolded the proteins using 8*M* urea (100 μ*M* protein concentration) and initiated the aggregation reaction by diluting the denaturant 10 times in a stopped flow mixer. The kinetics was monitored by following the changes in right-angle light scattering at 450 nm where the proteins do not absorb. The increase in light scattering intensity is proportional to the amount of protein aggregated. Dystrophin N-ABD aggregates at a much faster rate compared to utrophin N-ABD [Fig. 6(A)]. Both proteins showed typical nucleation—propagation kinetics, with a longer lag time for utrophin N-ABD compared to dystrophin N-ABD. These lag times which correspond to the formation of initial aggregation nuclei indicate that the utrophin N-ABD has a lesser tendency to aggregate compared to dystrophin N-ABD. At the end of the reaction, utrophin N-ABD refolded by about 24%, whereas dystrophin N-ABD refolded by only 4% [Fig. 6(B)]. These aggregation experiments indicate that utrophin N-ABD aggregates to a lesser extent than does dystrophin N-ABD despite having a lower stability.

Since the above aggregation reaction was initiated from the unfolded states, the aggregation propensities of the two proteins might be dictated by the inherent properties of the amino acid sequence rather than their thermodynamic stability. To exclude such a possibility, we used various computational programs[80,81] that predict the aggregation propensity of a protein based on its amino acid sequence and found that there is no difference in the aggregation propensity of the two polypeptide chains (Supporting Information Table), which is consistent with their high sequence similarity (82%) [Fig. 1(A)].

Utrophin N-ABD mutants have decreased stability similar to that of dystrophin disease-causing mutants

To determine whether utrophin mutations behave similar to disease-causing mutations in dystrophin, we introduced three missense mutations L70R, A184D, and Y246N at analogous positions to those of the dystrophin mutations, L54R, A168D, and Y231N. Like dystrophin mutants,[42] utrophin mutants aggregate significantly. When expressed in *E. coli*, the three mutants were found only in inclusion bodies, in contrast to the wild-type (WT) utrophin N-ABD, which was predominantly expressed as a soluble protein [Fig. 7(A)]. The three mutants were purified by solubilizing inclusion bodies in 8*M* urea and using Ni-affinity chromatography [Fig. 7(B)]. When the denaturant concentration was diluted, the mutants aggregate by 99%. This behavior is similar to that of the disease-causing dystrophin mutations.[42] We used thioflavin T and congo red dyes to probe the structure of these aggregates, which are two commonly used dyes that are known to bind to amyloid-like cross-β structure.[82,83] An increase in thioflavin T fluorescence and a red shift in congo red absorption spectrum are two signatures of the cross-β structure in the protein aggregates. Upon adding thioflavin T to preformed mutant

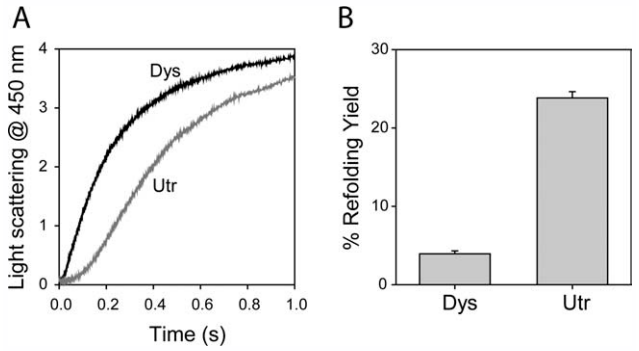

Figure 6

A. Protein aggregation monitored by changes in the right-angle light scattering at 450 nm initiated by diluting the denaturant 10 times starting from unfolded N-ABDs (100 μ*M*; 8*M* urea). Black and gray curves correspond to dystrophin (Dys) and utrophin (Utr) N-ABDs, respectively. **B**. Refolding yields of dystrophin and utrophin N-ABDs.

aggregates, the dye fluorescence intensity increased by on average 16 times compared with that in the buffer or in the presence of the native WT protein [Fig. 7(C)]. This increase is much higher than that observed for aggregates of the WT protein, indicating that the mutations enhance the cross-β nature of the aggregates. Upon adding congo red to preformed mutant aggregates, the dye absorption spectrum was red shifted on average by 70 nm [Fig. 7(D)]. Similar to thioflavin T fluorescence, the observed red shift for mutant aggregates is much higher than that observed for the WT protein aggregates. These two dye binding assays indicate that the predominant structure in utrophin N-ABD mutant aggregates is very similar to the cross-β structure observed earlier for dystrophin N-ABD aggregates.[42]

Because most of the mutant proteins were expressed as inclusion bodies and purified under denaturing conditions (8*M* urea), it was difficult to obtain high quantities of soluble proteins after refolding that were necessary to carry out urea melts. Hence, we used thermal melts to measure the differences in their stability. We first confirmed that the urea unfolding and refolding of the WT protein is reversible. The CD spectrum of the refolded WT exactly overlaps with that of the freshly purified WT [Fig. 8(A), top panel]. Also, refolded WT melted with the same T_m as that of the freshly purified WT [Fig. 8(B), top panel]. These observations indicate that the utrophin N-ABD reaches the same authentic native conformation after refolding from its denatured state at 8*M* urea. In the case of refolded mutants, L70R and A184D did not show a well-defined negative CD band at 222 nm compared with the WT protein [Fig. 8(A)], indicating a decrease in their α-helical content. The third mutant Y246N showed clear negative CD bands at 222 and 208 nm, similar to the WT utrophin, suggesting that Y246N has a similar structure to the WT protein. We were unable to calculate the mean residue ellipticity for mutants, as the soluble protein concentrations we could obtain were less than 1 μ*M* which were difficult to accurately quantitate using either absorbance at 280 nm or micro-BCA assay. However, we could use the ratio of CD values at 222 and 208 nm to qualitatively determine the loss of native α-helical structure. The ratios were 0.80, 0.75, and 0.93 for L70R, A184D, and Y246N mutants, respectively, whereas it was 0.94 for the WT protein. These values reconfirm that L70R and A184D have decreased α-helical content, whereas Y246N has an α-helical content similar to that of the WT protein. The behavior of all three utrophin mutants is very similar to that observed earlier for analogous mutations in dystrophin N-ABD,[42] where L54R and A168D mutants have decreased α-helicity and the Y231N mutant has a similar native structure as that of the WT protein. In terms of thermal melts, the two mutants L70R and A184D did not show a clear cooperative sigmoidal melt with the increase in solution temperature [Fig. 8(B)]. The lack of a cooperative unfolding

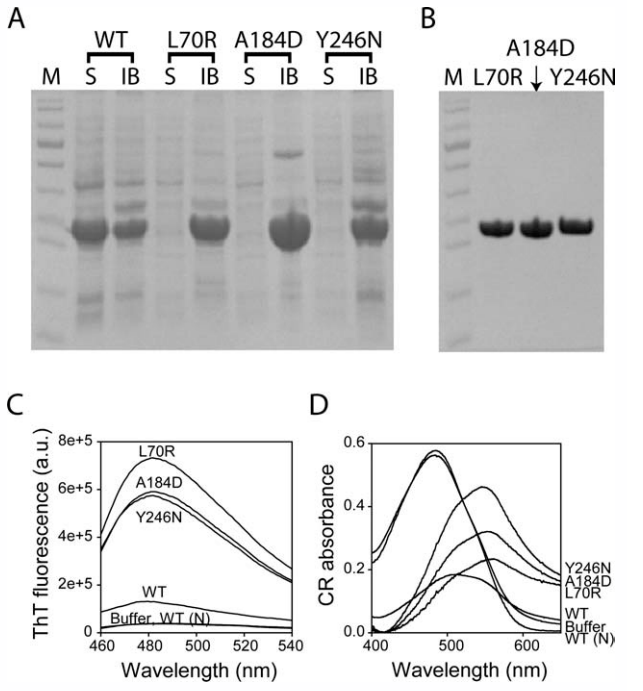

Figure 7

A. SDS-PAGE of WT utrophin N-ABD and its mutants expressed in *E coli*. S and IB represent the protein content in solution phase and in inclusion bodies respectively. **B**. SDS-PAGE of purified utrophin N-ABD mutants. In panels **A** and **B**, lane M corresponds to the protein molecular weight markers (bottom to top: 11, 17, 26, 34, 43, 56, 72, 96, 130, and 170 kDa, respectively). **C**. Increased thioflavin T (ThT) fluorescence when bound to protein aggregates. The figure shows the fluorescence in buffer, in the presence of soluble native WT protein (WT (N)), and when bound to aggregates (WT and mutants). **D**. Red shift in congo red (CR) absorption spectra upon binding to protein aggregates. The figure shows the spectra in buffer, in the presence of soluble native WT protein (WT (N)), and when bound to aggregates (WT and mutants).

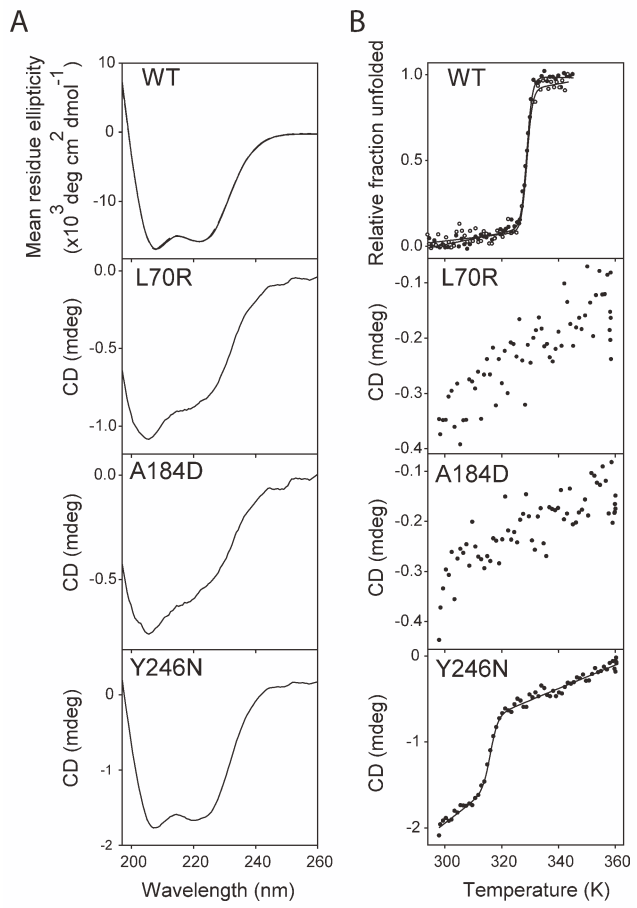

Figure 8

A. CD spectra of WT utrophin N-ABD and its mutants refolded from their denatured states at 8*M* urea. **B**. Thermal melts of WT and mutants measured by CD at 222 nm recorded as a function of increasing temperature. Top panels of **A** and **B** show the overlapping data of freshly purified WT and refolded WT from its denatured state at 8*M* urea.

indicates the absence of a stable structure and that the proteins probably exist in a molten globule-like conformation. In contrast, the Y246N mutant showed a clear cooperative temperature melt, indicating the presence of a stable structure. However, its T_m is 7°C less than that observed for the WT utrophin N-ABD, indicating decreased stability of the mutant. These results indicate that the utrophin mutants behave similar to dystrophin disease-causing mutants in terms of protein stability.[42]

DISCUSSION

Utrophin expression is upregulated in MD patients and in dystrophin-deficient *mdx* mice; however, it does not prevent progressive muscle degeneration.[15,26,31,84–87] Deletion of utrophin in the *mdx* mouse that lacks dystrophin, the so-called dystrophin-utrophin double knockout *dko* mice, results in very severe symptoms of MD similar to those of human DMD patients.[88,89] This suggests that in mice, and probably to some extent in humans, utrophin does have some protective effect on muscle integrity. Expression of the utrophin gene in muscles rescued the *dko* mice from MD symptoms and premature death.[17,48] Similar overexpression of utrophin using gene transfer methods rescued *mdx* mice from MD.[16,45,47] These ground-breaking animal experiments indicated that utrophin and dystrophin might play synergistic roles *in vivo* and that utrophin can compensate for the loss of dystrophin. Therefore, a number of therapies have been proposed to increase utrophin levels in muscles to treat MD patients.[20,23,90] The main advantage of using utrophin is its minimal immunological response because it is expressed at low levels even in those MD patients who completely lack dystrophin[19,20,26,47,87,91] Despite the animal experiments and proposed therapies, a complete understanding of how utrophin is similar to or different from dystrophin in terms of protein structure and related biophysical properties is lacking, and such an understanding will aid in designing better and more stable compensatory gene products for therapeutic use.

Decreased *in vivo* half-life of utrophin may result from its decreased stability

In recent studies, utrophin has been shown to interact with dystrophin-associated proteins which include the sarcolemmal glycoprotein complex[32–35] and binds to actin with a binding affinity similar to that of dystrophin,[36] thus linking actin to the sarcolemma.[34] However, when dystrophin and utrophin DNAs were expressed in animal models using gene transfer methods, dystrophin expression lasted longer compared with that of utrophin, indicating that utrophin has a shorter half-life.[16,21,38,39] One reason behind this difference may be because of the decreased stability (Fig. 3) and faster unfolding (Fig. 4) of utrophin compared to dystrophin. Decreased stability increases the nonfunctional unfolded state population at equilibrium. Increased unfolding rate increases the transient population of the unfolded state compared with the native state. Increased unfolded state population results in increased protein degradation by proteasome and other proteases resulting in depletion of the functional protein concentration, because the extent of proteolysis depends on the stability of the substrate protein.[79,92–95] Accordingly, less stable utrophin N-ABD is more prone to proteolysis compared with dystrophin N-ABD (Fig. 5). A recently published study on the full-length proteins[56] agrees with these inferences drawn based on the stability differences of N-ABDs. In addition, a few other studies suggest the role of proteasome and proteases in controlling the levels of dystrophin and utrophin *in vivo*.[96–98] Based on these observations, one possible method of designing stable utrophin constructs to

compensate the functional dystrophin loss seen in MD patients might be through increasing the stability of N-ABDs by protein engineering methods, which might increase the *in vivo* half-life of utrophin.

Utrophin may aggregate less than dystrophin

It has recently been shown that a possible physical mechanism by which missense mutations in dystrophin trigger disease is by inducing protein aggregation.[42,43] In contrast, utrophin possesses significant advantage over dystrophin in terms of protein aggregation. Starting from an unfolded state (analogous to a newly synthesized peptide by the ribosome machinery), utrophin N-ABD aggregates to a lesser extent despite having decreased stability compared with dystrophin N-ABD (Fig. 6). This behavior contradicts the general presumption in protein literature that less stable proteins aggregate to a higher extent.[99–101] We confirmed that the aggregation of the two proteins is not dictated by the primary structure of the polypeptide chains.

One possible explanation for this behavior is that while refolding, dystrophin N-ABD might misfold to a larger extent compared to utrophin N-ABD. The higher denaturant *m*-value for dystrophin N-ABD indicates that it is more compact than utrophin N-ABD [Figs. 3(A,B), and Table I], which might arise from the strength of the inter-CH-domain interactions in the two proteins. In such a case, there will be a higher chance for incorrect docking of the two CH domains during the folding of dystrophin N-ABD, which might result in increased aggregation of dystrophin N-ABD compared to utrophin N-ABD (Supporting Information Table).

Possible role of utrophin deficiency in disease mechanisms

Utrophin is the closest homologue of dystrophin and is believed to function in a similar way to dystrophin.[5,34] Having high sequence, structural and functional similarity, it is highly likely that mutations in utrophin behave similar to dystrophin mutations. It has been recently shown that disease-causing mutations in dystrophin decrease its stability and lead to its aggregation,[42,43] resulting in decreased dystrophin levels seen in MD patients.[102,103] Our results presented here indicate that the utrophin mutations behave similar to dystrophin mutations in terms of instability and aggregation and, therefore, might lead to decreased utrophin concentration *in vivo*. Since utrophin expression is quite low in skeletal muscles in the presence of dystrophin, decreased utrophin levels might not trigger MD. In the absence of dystrophin, utrophin expression is upregulated,[104] and hence any factors that diminish the utrophin concentration might lead to the increased severity of disease progression. Utrophin, being a large protein containing 3433 residues and its gene containing 900 Kb,[105] there will be a higher chance for the occurrence of sporadic mutations *in vivo* compared to proteins of a smaller size, and any such mutations that decrease its stability might make utrophin less effective in compensating the dystrophin loss. Alternatively, utrophin mutations might affect muscle development in the fetus and/or affect synapse transmission at myotendinous and neuromuscular junctions where utrophin plays a critical role. In support, utrophin deficiency and its mutations have recently been implicated in diseases such as myasthenia gravis, myelinopathies, cancer and diseases associated with the central nervous system.[106–111] Given the observation that utrophin is naturally upregulated in DMD and *mdx*, it is likely to have a significant protective effect. Mutations in utrophin that increase the instability of the protein could therefore be significant and detrimental modifiers in DMD. Mutations in potential modifier genes such as utrophin, which to date are unmapped, could contribute to the variation in phenotype and disease progression seen in DMD patients.

Inter-CH-domain interactions might control the stability and aggregation of tandem-repeat CH domains

Dystrophin and utrophin N-ABDs contain two CH domains linked by an α-helix [Fig. 1(B)]. Available X-ray crystal structures indicate that the orientation of CH domains around the central α-helix might differ between the two proteins [Fig. 1(C)], although the structures of individual CH domains are identical [Fig. 1(D)]. Results from the denaturant melts [Figs. 3(A,B), and Table I] indicate that utrophin N-ABD is less stable (lower ΔG) and has less buried surface area (lower *m*-value) compared to dystrophin N-ABD, which might indicate that the utrophin N-ABD has weaker inter-domain interactions. Consistently, recent results on the solution conformation of utrophin N-ABD indicates that it is an open, extended conformation where the two CH domains are far apart.[63] As discussed above, stronger inter-CH-domain interactions in dystrophin N-ABD might explain why dystrophin N-ABD aggregates to a higher extent compared to utrophin N-ABD because of the possibility of incorrect docking of the two CH domains during folding. These observations suggest that the stability, unfolding, and the aggregation behavior of tandem-CH-domains might be controlled by the inter-domain interactions between the two CH domains.

ACKNOWLEDGMENTS

We gratefully acknowledge the help from the Rocky Mountain 900 MHz NMR Facility (funded by the NIH instrumentation Grant P41GM068928) and Biophysics Core, University of Colorado Anschutz Medical Campus

in carrying out this work. We thank Javier Cabello-Villegas, Philip Reigan, Ruth Nussinov, Deborah Wuttke for helpful discussions, and Walter Englander and John Carpenter for their critical reading of the manuscript. This work was funded by the American Heart Association (to KMGM), a Jane and Charlie Butcher grant in Genomics and Biotechnology (to KMGM), the ALSAM Foundation through the Skaggs Scholars Program (to KMGM), and the Medical Research Council, UK (to SJW).

REFERENCES

1. Emery AEH. The muscular dystrophies. Lancet 2002;359:687–695.
2. Hoffman EP, Brown J, Robert H., Kunkel LM. Dystrophin: the protein product of the Duchenne muscular dystrophy locus. Cell 1987;51:919–928.
3. Winder SJ. Dystrophin and utrophin: the missing links! FEBS Lett 1995;369:27–33.
4. Roberts RG. Protein family review: dystrophins and dystrobrevins. Gen Biol 2001;2:reviews3006.3001–3006.3007.
5. Ervasti JM. Dystrophin, its interactions with other proteins, and implications. Biochim Biophys Acta 2007;1772:108–117.
6. Roberts RG, Borrow M, Bentley DR. Point mutations in the dystrophin gene. Proc Natl Acad Sci USA 1992;89:2331–2335.
7. Roberts RG, Gardner RJ, Bobrow M. Searching for the 1 in 2,400,000: a review of dystrophin gene point mutations. Hum Mutat 1994;4:1–11.
8. Prior TW, Bartolo C, Pearl DK, Papp AC, Snyder PJ, Sedra MS, Burghes AHM, Mendell JR. Spectrum of small mutations in the dystrophin coding region. Am J Hum Genet 1995;57:22–33.
9. Sitnik R, Campiotto S, Vainzof M, Pavanello RC, Takata RI, Zatz M, Passos-Bueno MR. Novel point mutations in the dystrophin gene. Human Mutat 1997;10:217–222.
10. Muntoni F, Torelli S, Ferlini A. Dystrophin and mutations: One gene, several proteins, multiple phenotypes. Lancet Neurol 2003;2:731–740.
11. Aaartsma-Rus A, van Deutekom JCT, Fokkema IF, van Ommen G-JB, Den Dennen JT. Entries in the Leiden Duchenne muscular dystrophy mutation database: an overview of mutation types and paradoxical cases that confirm the reading-frame rule. Muscle Nerve 2006;34:135–144.
12. Love DR, Hill DF, Dickson G, Spurr NK, Byth BC, Marsden RF, Walsh FS, Edwards YH, Davies KE. An autosomal transcript in skeletal muscle with homology to dystrophin. Nature 1989;339:55–58.
13. Khurana TS, Hoffman EP, Kunkel L. Identification of a chromosome 6-encoded dystrophin-related protein. J Biol Chem 1990;265:16717–16720.
14. Tinsley JM, Blake DJ, Roche A, Fairbrother U, Riss J, Byth BC, Knight AE, Kendrick-Jones J, Suthers GK, Love DR, Edwards YH, Davies KE. Primary structure of dystrophin-related protein. Nature 1992;360:591–593.
15. Blake DJ, Weir A, Newey SE, Davies KE. Function and genetics of dystrophin and dystrophin-related proteins in muscle. Physiol Rev 2002;82:291–329.
16. Tinsley J, Deconinck N, Fisher R, Kahn D, Phelps S, Gillis J-M, Davies K. Expression of full-length utrophin prevents muscular dystrophy in *mdx* mice. Nature Med 1998;4:1441–1444.
17. Rafael JA, Tinsley JM, Potter AC, Deconinck AE, Davies KE. Skeletal muscle-specific expression of a utrophin transgene rescues utrophin-dystrophin deficient mice. Nat Genet 1998;19:79–82.
18. Chamberlain JS. Gene therapy of muscular dystrophy. Hum Mol Genet 2002;11:2355–2362.
19. van Deutekom JCT, van Ommen G-JB. Advances in Duchenne muscular dystrophy gene therapy. Nat Rev Genet 2003;4:774–783.
20. Miura P, Jasmin BJ. Utrophin upregulation for treating Duchenne or Becker muscular dystrophy: How close are we? Trends Mol Med 2006;12:122–129.
21. Deol JR, Danialou G, Larochelle N, Bourget M, Moon J-S, Liu A-B, Gilbert R, Petrof BJ, Nalbantoglu J, Karpati G. Successful compensation for dystrophin deficiency by a helper-dependent adenovirus expressing full-length utrophin. Mol Ther 2007;15:1767–1774.
22. Odom GL, Gregorevic P, Allen JM, Finn E, Chamberlain JS. Microutrophin delivery through rAAV6 increases lifespan and improves muscle function in dystrophic dystrophin/utrophin-deficient mice. Mol Ther 2008;16:1539–1545.
23. Sonnemann KJ, Heun-Johnson H, Turner AJ, Baltgalvis KA, Lowe DA, Ervasti JM. Functional substitution by TAT-utrophin in dystrophin-deficient mice. PLoS Med 2009;6:e1000083.
24. Khurana TS, Watkins SC, Chafey P, Chelly J, Tome FMS, Fardeau M, Kaplan J-C, Kunkel LM. Immunolocalization and developmental expression of dystrophin related protein in skeletal muscle. Neuromusc Disord 1991;1:185–194.
25. Love DR, Morris GE, Ellis JM, Fairbrother U, Marsden RF, Bloomfield JF, Edwards YH, Slater CP, Parry DJ, Davies KE. Tissue distribution of the dystrophin-related gene product and expression in the *mdx* and *dy* mouse. Proc Natl Acad Sci USA 1991;88:3243–3247.
26. Helliwell TR, Man NT, Morris GE, Davies KE. The dystrophin-related protein, utrophin, is expressed on the sarcolemma of regenerating human skeletal muscle fibers in dystrophies and inflammatory myopathies. Neuromusc Disord 1992;2:177–184.
27. Blake DJ, Tinsley JM, Davies KE. Utrophin: a structural and functional comparison to dystrophin. Brain Pathol 1996;6:37–47.
28. Ohlendieck K, Ervasti JM, Matsumura K, Kahl SD, Leveille CJ, Campbell KP. Dystrophin-related protein is localized to neuromuscular junctions of adult skeletal muscle. Neuron 1991;7:499–508.
29. Gramolini AO, Jasmin BJ. Duchenne muscular dystrophy and the neuromuscular junction: the utrophin link. BioEssays 1997;19:747–750.
30. Moores CA, Kendrick-Jones J. Biochemical characterization of the actin-binding properties of utrophin. Cell Motil Cytoskeleton 2000;46:116–128.
31. Pons F, Augier N, Léger JOC, Robert A, Tomé FMS, Fardeau M, Voit T, Nicholson LVB, Mornet D, Léger JJ. A homologue of dystrophin is expressed at the neuromuscular junctions of normal individuals and DMD patients, and of normal and *mdx* mice: immunological evidence. FEBS Lett 1991;282:161–165.
32. Matsumura K, Ervasti JM, Ohlendieck K, Kahl SD, Campbell KP. Association of dystrophin-related protein with dystrophin-associated proteins in mdx mouse muscle. Nature 1992;360:588–591.
33. Winder SJ, Hemmings L, Maciver SK, Bolton SJ, Tinsley JM, Davies KE, Critchley DR, Kendrick-Jones J. Utrophin actin binding domain: analysis of actin binding and cellular targeting. J Cell Sci 1995;108:63–71.
34. Rybakova IN, Patel JR, Davies KE, Yurchenco PD, Ervasti JM. Utrophin binds laterally along actin filaments and can couple costameric actin with sarcolemma when overexpressed in dystrophin-deficient muscle. Mol Biol Cell 2002;13:1512–1521.
35. Ishikawa-Sakurai M, Yoshida M, Imamura M, Davies KE, Ozawa E. ZZ domain is essentially required for the physiological binding of dystrophin and utrophin to β-dystroglycan. Hum Mol Genet 2004;13:693–702.
36. Rybakova IN, Humston JL, Sonnemann KJ, Ervasti JM. Dystrophin and utrophin bind actin through distinct modes of contact. J Biol Chem 2006;281:9996–10001.
37. Prochniewicz E, Henderson D, Ervasti JM, Thomas DD. Dystrophin and utrophin have distinct effects on the structural dynamics of actin. Proc Natl Acad Sci USA 2009;106:7822–7827.
38. Squire S, Raymackers JM, Vandebrouck C, Potter A, Tinsley J, Fisher R, Gillis JM, Davies KE. Prevention of pathology in *mdx* mice by expression of utrophin: analysis using an inducible transgenic expression system. Hum Mol Genet 2002;11:3333–3344.

39. Ahmad A, Brinson M, Hodges BL, Chamberlain JS, Amalfitano A. *Mdx* mice inducibly expressing dystrophin provide insights into the potential of gene therapy for Duchenne muscular dystrophy. Hum Mol Genet 2000;9:2507–2515.
40. Keep NH, Winder SJ, Moores CA, Walke S, Norwood FLM, Kendrick-Jones J. Crystal structure of the actin-binding region of utrophin reveals a head-to-tail dimer. Structure 1999;7:1539–1546.
41. Norwood FL, Sutherland-Smith AJ, Keep NH, Kendrick-Jones J. The structure of the N-terminal actin-binding domain of human dystrophin and how mutations in this domain may cause Duchenne or Becker muscular dystrophy. Structure 2000;8:481–491.
42. Singh SM, Kongari N, Cabello-Villegas J, Mallela KMG. Missense mutations in dystrophin that trigger muscular dystrophy decrease protein stability and lead to cross-β aggregates. Proc Natl Acad Sci USA 2010;107:15069–15074.
43. Henderson DM, Lee A, Ervasti JM. Disease-causing missense mutations in actin binding domain 1 of dystrophin induce thermodynamic instability and protein aggregation. Proc Natl Acad Sci USA 2010;107:9632–9637.
44. Phelps SF, Hauser MA, Cole NM, Rafael JA, Hinkle RT, Faulkner JA, Chamberlain JS. Expression of full-length and truncated dystrophin mini-genes in transgenic mdx mice. Hum Mol Genet 1995;4:1251–1258.
45. Tinsley JM, Potter AC, Phelps SR, Fisher R, Trickett JI, Davies KE. Amelioration of the dystrophin phenotype of *mdx* mice using a truncated utrophin transgene. Nature 1996:349–353.
46. Deconinck N, Tinsley J, Backer FD, Fisher R, Kahn D, Phelps S, Davies K, Gillis J-M. Expression of truncated utrophin leads to major functional improvements in dystrophin-deficient muscles of mice. Nat Med 1997;3:1216–1221.
47. Gilbert R, Nalbantoglu J, Petrof BJ, Ebihara S, Guibinga GH, Tinsley JM, Kamen A, Massie B, Davies KE, Karpati G. Adenovirus-mediated utrophin gene transfer mitigates the dystrophin phenotype of mdx mouse muscles. Hum Gene Ther 1999;10:1299–1310.
48. Wakefield PM, Tinsley JM, Wood MJA, Gilbert R, Karpati G, Davies KE. Prevention of the dystrophic phenotype in dystrophin/utrophin-deficient muscle following adenovirus-mediated transfer of a utrophin minigene. Gene Therapy 2000;7:201–204.
49. Wang B, Li J, Xiao X. Adeno-associated virus vector carrying human minidystrophin genes effectively ameliorates muscular dystrophy in mdx mouse model. Proc Natl Acad Sci USA 2000;97:13714–13719.
50. Gregorevic P, Allen JM, Minami E, Blankenship MJ, Haraguchi M, Meuse L, Finn E, Adams ME, Froehner SC, Murry CE, Chamberlain JS. rAAV6-microdystrophin preserves muscle function and extends lifespan in severely dystrophic mice. Nat Med 2006;12:787–789.
51. Scott JM, Li S, harper SQ. Viral vectors for gene transfer of micro-, mini-, or full-length dystrophin. Neuromuscular Disord 2002;12:s23–s29.
52. Gregorevic P, Chamberlain JS. Gene therapy for muscular dystrophy—a review of promising progress. Expert Opin Biol Ther 2003;3:803–814.
53. Foster K, Foster H, Dickson JG. Gene therapy progress and prospects: Duchenne muscular dystrophy. Gene Ther 2006;13:1677–1685.
54. Muir LA, Chamberlain JS. Emerging strategies for cell and gene therapy of the muscular dystrophies. Expert Rev Mol Med 2009;11:e18.
55. Fairclough RJ, Bareja A, Davies KE. Progress in therapy for Duchenne muscular dystrophy. Exp Physiol 2011;96:1101–1113.
56. Henderson DM, Belanto JJ, Li B, Heun-Johnson H, Ervasti JM. Internal deletion compromises the stability of dystrophin. Hum Mol Genet 2011;20:2955–2963.
57. Le Rumeur E, Winder SJ, Hubert J-F. Dystrophin: more than just the sum of its parts. Biochim Biophys Acta 2010;1804:1713–1722.
58. Orlova A, Rybakova IN, Prochniewicz E, Thomas DD, Ervasti JM, Egelman EH. Binding of dystrophin's tandem calponin homology domain to F-actin is modulated by actin's structure. Biophys J 2001;80:1926.
59. Gimona M, Djinovic-Carugo K, Kranewitter WJ, Winder SJ. Functional plasticity of CH domains. FEBS Lett 2002;513:98–106.
60. Galkin VE, Orlova A, VanLoock MS, Egelman EH. Do the utrophin tandem calponin homology domains bind F-actin in a compact or extended conformation? J Mol Biol 2003;331:967–972.
61. Lehman W, Craig R, Kendrick-Jones J, Sutherland-Smith A. An open or closed case for the conformation of calponin homology domains on F-actin? J Muscle Res Cell Motility 2004;25:351–358.
62. Galkin VE, Orlova A, Salmazo A, Djinovic-Carugo K, Egelman EH. Opening of tandem calponin homology domains regulated their affinity for F-actin. Nat Struct Mol Biol 2010;17:614–616.
63. Lin AY, Prochniewicz E, James ZM, Svensson B, Thomas DD. Large-scale opening of utrophin's tandem calponin homology (CH) domains upon actin binding by an induced-fit mechanism. Proc Natl Acad Sci USA 2011;108:12729–12733.
64. Sutherland-Smith AJ, Moores CA, Norwood FLM, Hatch V, Craig R, Kendrick-Jones J, Lehman W. An atomic model for actin binding by the CH domains and spectrin-repeat modules of utrophin and dystrophin. J Mol Biol 2003;329:15–33.
65. Greenfield NJ. Using circular dichroism spectra to estimate protein secondary structure. Nat Protocols 2006;6:2876–2890.
66. Delaglio F, Grzesiek S, Vuister GW, Zhu G, Pfeifer J, Bax A. NMRPipe: a multidimensional spectral processing system based on UNIX pipes. J Biomol NMR 1995;6:277–293.
67. Santoro MM, Bolen DW. Unfolding free energy changes determined by the linear extrapolation method. 1. Unfolding of phenylmethanesulfonyl alpha-chymotrypsin using different denaturants. Biochemistry 1988;27:8063–8068.
68. Santoro MM, Bolen DW. A test of the linear extrapolation of unfolding free energy changes over an extended denaturant concentration range. Biochemistry 1992;31:4901–4907.
69. Chenna R, Sugawara H, Koike T, Lopez R, Gibson TJ, Higgins DG, Thompson JD. Multiple sequence alignment with the Clustal series of programs. Nucl Acids Res 2003;31:3497–3500.
70. Shatsky M, Nussinov R, Wolfson HJ. A method for simultaneous alignment of multiple protein structures. Protein Struct Funct Bioinform 2004;56:143–156.
71. Lakowicz JR. Principles of fluorescence spectroscopy. New York: Springer Science; 2006.
72. Daragan VA, Mayo KH. Motional model analyses of protein and peptide dynamics using ^{13}C and ^{15}N NMR relaxation. Prog NMR Spectroscopy 1997;31:63–105.
73. Myers JK, Pace CN, Scholtz JM. Denaturant m values and heat capacity changes: relation to changes in accessible surface areas of protein unfolding. Protein Sci 1995;4:2138–2148.
74. Kahana E, Flood G, Gratzer WB. Physical properties of dystrophin rod domain. Cell Motil Cytoskeleton 1997;36:246–252.
75. Ruszczak C, Mirza A, Menhart N. Differential stabilities of alternative exon-skipped rod motifs of dystrophin. Biochim Biophys Acta 2009;1794:921–928.
76. Legardinier S, Legrand B, Raguénès-Nicol C, Bondon A, Hardy S, Tascon C, Rumeur EL, Hubert J-F. A two-amino acid mutation encountered in Duchenne muscular dystrophy decreases stability of the rod domain 23 (R23) spectrin-like repeat of dystrophin. J Biol Chem 2009;284:8822–8832.
77. Krishna MMG, Englander SW. A unified mechanism for protein folding: predetermined pathways with optional errors. Protein Sci 2007;16:449–464.
78. Mirza A, Sagathevan M, Sahni N, Choi L, Menhart N. A biophysical map of the dystrophin rod. Biochim Biophys Acta 2010;1804:1796–1809.
79. Park C, Marqusee S. Probing the high energy states in proteins by proteolysis. J Mol Biol 2004;343:1467–1476.

80. Singh SM, Cabello-Villegas J, Hutchings RL, Mallela KMG. Role of partial protein unfolding in alcohol-induced protein aggregation. Protein Struct Funct Bioinform 2010;78:2625–2637.
81. Belli M, Ramazzotti M, Chiti F. Prediction of amyloid aggregation *in vivo*. EMBO Reports 2011;12:657–663.
82. Levine-III H. Thioflavine T interaction with synthetic Alzheimer's disease {beta}-amyloid peptides: Detection of amyloid aggregation in solution. Protein Sci 1993;2:404–410.
83. Klunk WE, Pettegrew JW, Abraham DJ. Quantitative evaluation of congo red binding to amyloid-like proteins with a beta-pleated sheet conformation. J Histochem Cytochem 1989;37:1273–1281.
84. Rafael JA, Townsend ER, Squire SE, Potter AC, Chamberlain JS, Davies KE. Dystrophin and utrophin influence fiber type composition and post-synaptic membrane structure. Hum Mol Genet 2000;9:1357–1367.
85. Pastoret C, Sebille A. Mdx mice show progressive weakness and muscle deterioration with age. J Neurol Sci 1995;129:97–105.
86. Tanabe Y, Esaki K, Nomura T. Skeletal muscle pathology in X chromosome-linked muscular dystrophy (mdx) mouse. Acta Neuropathol 1986;69:91–95.
87. Karpati G, Carpenter S, Morris GE, Davies KE, Guerin C, Holland P. Localization and quantitation of the chromosome 6-encoded dystrophin-related protein in normal and pathological human muscle. J Neuropathol Exp Neurol 1993;52:119–128.
88. Deconinck AE, Rafael JA, Skinner JA, Brown SC, Potter AC, Metzinger L, Watt DJ, Dickson JG, Tinsley JM, Davies KE. Utrophin-dystrophin-deficient mice as a model for Duchenne muscular dystrophy. Cell 1997;90:717–727.
89. Grady RM, Teng HB, Nichol MC, Cunningham JC, Wilkinson RS, Sanes JR. Skeletal and cardiac myopathies in mice lacking utrophin and dystrophin: a model for Duchenne muscular dystrophy. Cell 1997;90:729–738.
90. Odom GL, Gregorevic P, Chamberlain JS. Viral-mediated gene therapy for the muscular dystrophies: successes, limitations, and recent advances. Biochim Biophys Acta 2007;1772:243–262.
91. Ebihara S, Guibinga G-H, Gilbert R, Nalbantoglu J, Massie B, Karpati G, Petrof BJ. Differential effects of dystrophin and utrophin gene transfer in immunocompetent muscular dystrophy (mdx) mice. Physiol Genomics 2000;3:133–144.
92. Parsell DA, Sauer RT. The structural stability of a protein is an important determinant of its proteolytic susceptibility in *Escherichia coli*. J Biol Chem 1989;264:7590–7595.
93. Wang L, Kallenbach NR. Proteolysis as a measure of the free energy difference between cytochrome c and its derivatives. Protein Sci 1998;7:2460–2464.
94. Kim M-S, Song J, Park C. Determining protein stability in cell lysates by pulse proteolysis and Western blotting. Protein Sci 2009;18:1051–1059.
95. Ruschak AM, Religa TL, Breuer S, Witt S, Kay LE. The proteasome antechamber maintains substrates in the unfolded state. Nature 2010;467:868–871.
96. Cotton P, Poussard S, Mornet D, Brustis JJ, Mohammadpour M, Leger J, Ducastaing A. In vitro digestion of dystrophin by calcium-dependent proteases, calpains I and II. Biochimie 1992;74:565–570.
97. Courdier-Fruh I, Briguet A. Utrophin is a calpain substrate in muscle cells. Muscle Nerve 2006;33:753–759.
98. Badorff C, Lee G-H, Lamphear BJ, Martone ME, Campbell KP, Rhoads RE, Knowlton KU. Enteroviral protease 2A cleaves dystrophin: evidence of cytoskeletal disruption in an acquired cardiomyopathy. Nat Med 1999;5:320–326.
99. Chi EY, Krishnan S, Randolph TW, Carpenter JF. Physical stability of proteins in aqueous solution: mechanism and driving forces in nonnative protein aggregation. Pharmaceut Res 2003;20:1325–1336.
100. Mayer S, Rüdiger S, Ang HC, Joerger AC, Fersht AR. Correlation of levels of folded recombinant p53 in *Escherichia coli* with thermodynamic stability in vitro. J Mol Biol 2007;372:268–276.
101. Espargaró A, Castillo V, de Groot NS, Ventura S. The *in vivo* and *in vitro* aggregation properties of globular proteins correlate with their conformational stability: the SH3 case. J Mol Biol 2008;378:1116–1131.
102. Prior TW, Papp AC, Snyder PJ, Burghes AHM, Bartolo C, Sedra MS, Western LM, Mendell JR. A missense mutation in the dystrophin gene in a Duchenne muscular dystrophy patient. Nat Genet 1993;4:357–360.
103. Hamed SA, Sutherland-Smith AJ, Gorospe JRM, Kendrick-Jones J, Hoffman EP. DNA sequence analysis for structure/function and mutation studies in Becker muscular dystrophy. Clin Genet 2005;68:69–79.
104. Fisher R, Tinsley JM, Phelps SR, Squire SE, Townsend ER, Martin JE, Davies KE. Non-toxic ubiquitous over-expression of utrophin in the *mdx* mouse. Neuromusc Disorder 2001;11:713–721.
105. Pearce M, Blake DJ, Tinsley JM, Byth BC, Campbell L, Monaco AP, Davies KE. The utrophin and dystrophin genes share similarities in genomic structure. Hum Mol Genet 1993;2:1765–1772.
106. Ito H, Yoshimura T, Satoh A, Takino H, Tsujihata M, Nagataki S. Immunohistochemical study of utrophin and dystrophin at the motor end-plate in myasthenia gravis. Acta Neuropathol 1996;92:14–18.
107. Sieb JP, Kraner S, Rauch M, Steinlein OK. Immature end-plates and utrophin deficiency in congenital myasthemic syndrome caused by ϵ-AChR subunit truncating mutations. Hum Genet 2000;107:160–164.
108. Barghorn A, Speel EJM, Farspour B, Saremaslani P, Schmid S, Perren A, Roth J, Heitz PU, Komminoth P. Putative tumor suppressor loci at 6q22 and 6q23–q24 are involved in the malignant progression of sporadic endocrine pancreatic tumors. Am J Pathol 2001;158:1903–1911.
109. Nagarajan R, Le N, Mahoney H, Araki T, Milbrandt J. Deciphering peripheral nerve myelination by using Schwann cell expression profiling. Proc Natl Acad Sci USA 2002;99:8998–9003.
110. Knuesel I, Riban V, Zuellig RA, Schaub MC, Grady RM, Sanes JR, Fritschy J-M. Increased vulnerability to kainate-induced seizures in utrophin-knockout mice. Eur J Neurosci 2002;15:1474–1484.
111. Li Y, Huang J, Zhao Y-L, He J, Wang W, Davies KE, Nosé V, Xiao S. *UTRN* on chromosome 6q24 is mutated in multiple tumors. Oncogene 2007;26:6220–6228.
112. Mallela K, Singh S, Molas J, Cabello-Villegas J, Kongari N. Protein stability, folding, and aggregation of the N-terminal actin binding domains of dystrophin and utrophin. Protein Sci 2010;19(S1):180.